Bimodal Molecular Weight Distribution in Carbocationic Systems with Free Ions and Ion Pairs of Equal Reactivities but Different Lifetimes

Krzysztof Matyjaszewski,*,† Ryszard Szymanski,‡ and Mircea Teodorescu†

Department of Chemistry, Carnegie Mellon University, 4400 Fifth Avenue, Pittsburgh, Pennsylvania 15213, and Center of Molecular and Macromolecular Studies, Polish Academy of Sciences, Sienkiewicza 112, 90-363 Lodz, Poland

Received May 17, 1994; Revised Manuscript Received September 21, 1994®

ABSTRACT: Monte Carlo calculations and numerical integrations are used to study molecular weight distribution (MWD) in carbocationic polymerization and to illustrate the effect of equilibrium constants, rate constants, and concentration of common ions on MW and MWD. It is demonstrated that bimodal molecular weight distribution is obtained when exchange between ions and ion pairs of similar reactivities is slow and their lifetimes are sufficiently different. Bimodal MWD is converted to narrow (Poisson) distribution in the presence of salts with common ions; molecular weights in these systems grow linearly with conversion like in living polymerization.

Introduction

A chain polymerization with a variety of active species propagating simultaneously may yield polymers with a broad or a polymodal molecular weight distribution (MWD). The intuitive requirement for polymodality is a difference in reactivities of various active species, providing that the rate of exchange is lower than the rate of propagation. Detailed theoretical and experimental studies have been reported on the anionic polymerization of alkenes in which free ions are much more reactive than ion pairs.[1,2] The breadth of MWD was used to estimate the rate constants of exchange between free ions and ion pairs.[2,3] In these systems free ions are much more reactive than contact ion pairs (the ratio of rate constants approaches $k^-/k^\pm \approx 100\,000$), dissociation constants are rather small ($K_D \approx 10^{-7}$ mol/L), and rate constants of association are nearly diffusion controlled ($k_{assoc} \approx 10^9$ mol^{-1}·L·s^{-1}).[4] MWD in these systems is usually slightly broader than expected for a Poisson distribution ($M_w/M_n \approx 1.1$) but always monomodal.

A bimodal molecular weight distribution is very often observed in carbocationic polymerization.[5-7] It seems that high molecular weight (HMW) peak ($M_n > 100\,000$) remains fairly constant or decreases (both M_n and relative intensity) with conversion, whereas low molecular weight (LMW) peak ($10\,000 > M_n > 1000$) continuously increases with conversion. There are only a few data on the MWD of each separate peak, but it seems that the HMW peak has the most probable distribution ($M_w/M_n \approx 2$), whereas the polydispersity of LMW peak varies but can be very narrow ($M_w/M_n < 1.2$). It was also observed that addition of salts with common ions suppresses the HMW fraction but practically does not affect the LMW fraction.[5-7] Thus, it was concluded that the HMW fraction is formed by free ions. The origin of the LMW fraction is still under dispute. A new mechanism of propagation that might not involve "normal" carbocations was proposed. Some variations of the structure of species including covalent (pseudocationic mechanism), onium ions or obscure stabilization of carbenium ions were suggested.[8-10]

We have consistently tried to ascribe bimodal MWD in these systems to "normal" carbocationic free ions and ion pairs which might be in equilibrium with some dormant species such as covalent esters or onium ions.[11-13] The main difficulty in this theory is a nearly identical reactivity of free ions and ion pairs in most cationic systems. This was found in model studies as well as in polymerization.[14-16] This is in contrast to carbanionic systems and can be assigned to differences in interionic distances and relative solvation states of ions and ion pairs in both systems.[14,17]

Thus, is it possible to observe bimodal MWD in systems in which both propagating species have the same reactivities? We tentatively explain bimodality by differences in lifetimes of both species.[13] In this paper, we present results of Monte Carlo simulation and numerical integration of differential equations for a few systems in which covalent species are inactive and reactivities of free ions and ion pairs are identical and all species are in dynamic equilibrium. This approach has been used previously by one of us to verify Penczek's hypothesis on the effect of nucleophiles on polydispersities in carbocationic systems.[18] Calculations demonstrate that the shape and breadth of molecular weight distribution depends on relative rates of exchange between dormant and active species and on lifetimes of ions and ion pairs even if they have exactly the same reactivities.

Results and Discussion

Scheme 1 presents the propagation step in a typical carbocationic system:

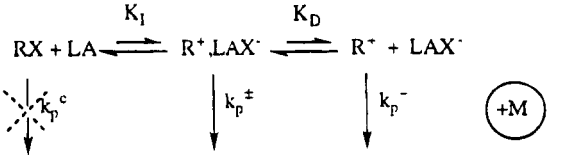

(1)

Covalent species are usually activated by Lewis acids to form ion pairs. Ion pairs dissociate to free ions. Covalent species are considered to be inactive ($k_p^c = 0$). The rate constants of propagation on ions and ion pairs are assumed to be equal one to another ($k_p^+ = k_p^\pm$). The equilibrium constant between covalent species and ion

† Carnegie Mellon University.
‡ Polish Academy of Sciencs.
® Abstract published in *Advance ACS Abstracts,* November 15, 1994.

0024-9297/94/2227-7565$04.50/0

Table 1. Number Average Degrees of Polymerization (DP_n) and Polydispersities (Disp = DP_w/DP_n) Calculated by the Numerical Integrations at Conversions 10%, 50%, and 90% as Well as by the Monte Carlo Simulations (MC, 90% conversion only) for Systems with Variable Dissociation and Ionization Equilibria[a]

no.	K_D (M)	k_{diss} (s^{-1})	K_I (M^{-1})	k_r (s^{-1})	k_i ($M^{-1}\cdot s^{-1}$)	[IP]/[I]$_0$	[FI]/[I]$_0$	DP_n(10)	Disp(10)	DP_n(50)	Disp(50)	DP_n(90)	Disp(90)	$DP_n(90)^{MC}$	$Disp(90)^{MC}$
1	10^{-7}	10^2	10^{-7}	10^3	10^4	10^{-8}	3×10^{-7}	3258	19.8	2426	21	1371	27.3	1043	36.5
2	10^{-7}	10^2	10^{-7}	10^5	10^{-2}	10^{-8}	3×10^{-7}	69	848	85.3	540.2	107.2	316.1	119	313
3	10^{-7}	10^2	10^{-7}	10^7	1	10^{-8}	3×10^{-7}	38.1	1525	64	719.8	96.1	351.6	90.7	401
4	10^{-7}	10^2	10^{-7}	10^9	10^2	10^{-8}	3×10^{-7}	38.1	1526	64	722	96	351.9	89.8	387
5	10^{-7}	10^2	10^{-5}	10^3	10^{-2}	10^{-6}	3×10^{-6}	404.3	13.2	330	13	218	14.6	211	14
6	10^{-7}	10^2	10^{-5}	10^5	1	10^{-6}	3×10^{-6}	14.3	324.4	50	73.1	90	30.4	89.3	29.9
7	10^{-7}	10^2	10^{-5}	10^7	10^2	10^{-6}	3×10^{-6}	11.03	415	50	73.1	90	30.3	91.4	30.3
8	10^{-7}	10^2	10^{-5}	10^9	10^4	10^{-6}	3×10^{-6}	11.1	415.7	50	73.1	90	30.4	91.3	29.3
9	10^{-7}	10^2	10^{-3}	10^3	1	10^{-4}	3×10^{-5}	131	3.08	123.4	2.934	110.5	2.889	109	2.81
10	10^{-7}	10^2	10^{-3}	10^5	10^2	10^{-4}	3×10^{-5}	10.3	15.4	50	3.337	90	1.955	90.2	1.98
11	10^{-7}	10^2	10^{-3}	10^7	10^4	10^{-4}	3×10^{-5}	10	15.5	50	3.298	90	1.939	91.4	1.9
12	10^{-7}	10^2	10^{-3}	10^9	10^6	10^{-4}	3×10^{-5}	10	15.5	50	3.297	90	1.9	92	1.9
13	10^{-6}	10^3	10^{-7}	10^3	10^{-4}	10^{-8}	10^{-6}	9675	3.919	7343	4.053	4107	5.32	4130	5.32
14	10^{-6}	10^3	10^{-7}	10^5	10^{-2}	10^{-8}	10^{-6}	204.5	90.5	200.2	74.6	198	55.8	196	54.2
15	10^{-6}	10^3	10^{-7}	10^7	1	10^{-8}	10^{-6}	106	177	127.3	117	150.3	72.8	151	72.2
16	10^{-6}	10^3	10^{-7}	10^9	10^2	10^{-8}	10^{-6}	105	178	125.5	117.5	150	73.15	99	111
17	10^{-6}	10^3	10^{-5}	10^3	10^{-2}	10^{-6}	10^{-5}	1053	3.608	828	3.692	492	4.674	493	4.7
18	10^{-6}	10^3	10^{-5}	10^5	1	10^{-6}	10^{-3}	26	65.7	54.1	26.6	90.3	12.21	91	12.2
19	10^{-6}	10^3	10^{-5}	10^7	10^2	10^{-6}	10^{-5}	16.7	103.3	50.5	28	90	12.1	91	11.8
20	10^{-6}	10^3	10^{-5}	10^9	10^4	10^{-6}	10^{-3}	16.5	104.3	50.5	28	90	12.1	91	11.6
21	10^{-6}	10^3	10^{-3}	10^3	1	10^{-4}	10^{-4}	196	2.466	172.5	2.465	134.1	2.726	134.2	2.73
22	10^{-6}	10^3	10^{-3}	10^5	10^2	10^{-4}	10^{-4}	11.1	10.13	50	2.579	90	1.646	90.2	1.65
23	10^{-6}	10^3	10^{-3}	10^7	10^4	10^{-4}	10^{-4}	10	10.5	50	2.51	90	1.622	91.8	1.6
24	10^{-6}	10^3	10^{-3}	10^9	10^6	10^{-4}	10^{-4}	10.1	10.5	50	2.519	90	1.622	92	1.6
25	10^{-5}	10^4	10^{-7}	10^3	10^{-4}	10^{-8}	3×10^{-6}	30106	2.178	23170	2.257	12760	3.01	11570	3.27
26	10^{-5}	10^4	10^{-7}	10^5	10^{-2}	10^{-8}	3×10^{-6}	592.1	11.12	537	9.79	444	8.79	445	8.81
27	10^{-5}	10^4	10^{-7}	10^7	1	10^{-8}	3×10^{-6}	295	20.34	306.9	15.6	301.9	11.8	500	7.12
28	10^{-5}	10^4	10^{-7}	10^9	10^2	10^{-8}	3×10^{-6}	294.7	20.34	304.9	15.67	300.5	11.8	163	21.8
29	10^{-5}	10^4	10^{-5}	10^3	10^{-2}	10^{-6}	3×10^{-5}	3098	2.167	2405	2.244	1353	2.965	1357	2.98
30	10^{-5}	10^4	10^{-5}	10^5	1	10^{-6}	3×10^{-5}	66	998	81.7	6.87	101.3	4.582	101.3	4.59
31	10^{-5}	10^4	10^{-5}	10^7	10^2	10^{-6}	3×10^{-5}	35.5	16.9	60.8	8.41	93.2	4.608	93	4.57
32	10^{-5}	10^4	10^{-5}	10^9	10^4	10^{-6}	3×10^{-5}	35.1	17	60.6	8.43	92.9	4.61	91	4.66
33	10^{-5}	10^4	10^{-3}	10^3	1	10^{-4}	3×10^{-4}	397	2.095	329	2.156	216	2.658	216	2.66
34	10^{-5}	10^4	10^{-3}	10^5	10^2	10^{-4}	3×10^{-4}	13.9	4.679	50.5	1.864	90	1.355	90	1.35
35	10^{-5}	10^4	10^{-3}	10^7	10^4	10^{-4}	3×10^{-4}	10.9	5.252	50	1.741	90	1.305	91	1.3
36	10^{-5}	10^4	10^{-3}	10^9	10^6	10^{-4}	3×10^{-4}	10.8	5.256	50	1.74	90	1.305	91	1.29

[a] $[M]_0$ = 1 mol/L, $[LA]_0$ = 0.1 mol/L; $[I]_0$ = 0.01 mol/L; k_p^c = 0 $mol^{-1}\cdot L\cdot s^{-1}$, $k_p^+ = k_p^\pm = 10^5$ $mol^{-1}\cdot L\cdot s^{-1}$, $k_{assoc} = 10^9$ $mol^{-1}\cdot L\cdot s^{-1}$, $K_D = k_{diss}/k_{assoc}$; $K_I = k_i/k_r$; FI: free ions, IP: ion pairs.

pairs is defined by the ratio of the rate constant of ionization to that of recombination of counterions within the ion pair ($K_I = k_i/k_r$). The former bimolecular rate constant depends on the electrophilicity of the covalent species (RX) and the strength of the Lewis acid (MtX_n). The latter unimolecular rate constant depends on the stabilities of a carbocation (R^+) and that of the resulting complexed anion (MtX^-_{n-1}). The dissociation constant is defined by the ratio of the rate constants of dissociation of ion pair and that of association of free ions ($K_D = k_{dis}/k_{assoc}$). K_D depends mostly on "physical" parameters such as interionic distance and shape of ions, on solvent (dielectric constant, viscosity, specific solvation), and on temperature.

We simulated polymerization of styrene in CH_2Cl_2 solvent at the temperature range −20 to +20 °C, initiated by 1-phenylethyl chloride (a model of macromolecular covalent species) and activated by BCl_3 or $SnCl_4$. The latter Lewis acid has slightly higher strength which increases proportion of carbocations and the polymerization rate. It leads to $SnCl_5^-$ anion which can additionally act as a weak Lewis acid, ionize covalent species, aggregate, and form $SnCl_6^{2-}$ anions.[19] BCl_3 does not aggregate and can form only BCl_4^- anion. On the other hand, BCl_3 may add directly to alkenes via haloboration.[20] This process, more important at higher temperatures, reduces the concentration of Lewis acids and increases number of chains. Typical concentrations in polymerization[19-21] are $[M]_0$ = 1 mol/L, $[I]_0$ = 0.01 mol/L, and $[MtX_n]_0$ = 0.1 mol/L. These values were taken for calculations as shown in Table 1. The average molecular weights at complete conversion are $DP_n \approx 100$, as predicted for a controlled process, but molecular weight distributions are bimodal. Bimodality disappears in the presence of salts with common ions.[19-21]

Rate constants of propagation in most carbocationic polymerizations are in the range $k_p \approx 10^4-10^6$ $mol^{-1}\cdot L\cdot s^{-1}$. In Table 1 we used value $k_p^+ = k_p^\pm = 10^5$ $mol^{-1}\cdot L\cdot s^{-1}$ which is probably the closest to one in polymerization of styrene in CH_2Cl_2 at the discussed temperatures.[15,16] Covalent species are inactive, k_p^c = 0.

The estimated values of the dissociation process vary in the range $K_D \approx 10^{-7}-10^{-5}$ mol/L.[7,15] These values define the range of the dissociation rate constants by assuming that the association process is diffusion controlled, $k_{assoc} \approx 10^9$ $mol^{-1}\cdot L\cdot s^{-1}$ and $k_{diss} = k_{assoc}\cdot K_D \approx 10^2-10^4$ s^{-1}. In Table 1, we systematically varied K_D and k_{diss}. The first 12 entries are given for $K_D = 10^{-7}$ mol/L, the next 12 for $K_D = 10^{-6}$ mol/L, and the last 12 for $K_D = 10^{-5}$ mol/L.

The amount of ions (sum of ion pairs and free ions) can be assessed from the overall rate of propagation: $R_p = -d[M]/dt = k_p^+[M]\{[C^+] + [C^\pm]\}$. Typical values of the concentration of ionic species are in the case of polymerization of styrene initiated by 1-phenylethyl chloride ($[I]_0$ = 0.01 mol/L) and activated by either $SnCl_4$ or BCl_3 ($[LA]_0$ = 0.1 mol/L) in CH_2Cl_2 at temperatures from 20 to −20 °C are $[C^+] + [C^\pm] \approx 10^{-7}$ mol/L with approximately 50−80% contribution of free ions as

estimated from the common salt effects.[19] This leads to the approximate equilibrium constant of ionization $K_I \approx 10^{-5}$ mol^{-1}·L and dissociation constant $K_D \approx 10^{-6}$ mol/L.

Systems shown in Table 1 have been simulated varying not only dissociation parameters but also ionization equilibria and dynamics. For each value of K_D four different rate constants of recombination of ions pairs ($k_r = 10^3$, 10^5, 10^7, and 10^9 s^{-1}) and three different ionization equilibrium constants ($K_I = 10^{-7}$, 10^{-5}, and 10^{-3} mol^{-1}·L) have been chosen to determine the effect of both position of equilibrium and dynamics on molecular weights and molecular weight distribution.

Table 1 presents average values of molecular weights and overall polydispersities obtained from the numerical integrations of the differential equations (cf. Appendix) at different conversions (10%, 50%, and 90%) and those from the Monte Carlo simulations (at 90% conversion) for systems with variable dissociation and ionization equilibria and dynamics. The results of the numerical integrations and the Monte Carlo simulations are in very good agreement. Some deviations in the Monte Carlo calculations might be ascribed to the insufficient number of molecules taken for the simulation (cf. Appendix). Rate constants of the addition of the monomeric carbocations to alkenes (initiation) were assumed to be the same as propagation, and the ionization and dissociation equilibria the same for initiator as for the growing chain end. There is some information from model studies that this is a justified assumption.[19,21]

For fast initiation, the average values of DP_n = 10, 50, and 90 should be observed at conversions 10%, 50%, and 90%, correspondingly. As seen in Table 1, some DP_n values are much larger than expected and polydispersities extremely broad. This is due to the slow dynamics of exchange and has to be systematically explained not only by analyzing the overall numerical values of DP_n and polydispersities but also by inspecting shapes of MWD.

Effect of Conversion. Effect of conversion on the evolution of molecular weights and polydispersities is shown in Figures 1 and 2. Figure 1a,b shows experimental results obtained with styrene (1 mol/L) at −20 °C in CH_2Cl_2, using 1-phenylethyl chloride (0.01 mol/L), $SnCl_4$ (0.1 mol/L), and BCl_3 (0.1 mol/L) as initiating systems, respectively. With $SnCl_4$ polymerization is faster, the overall proportion of ions is higher, and proportion of ion pairs also higher. In Figure 1a low molecular weight oligomers are well resolved and then they merge to one peak at higher molecular weight. The degree of polymerization of LMW peak increases clearly with conversion in Figures 1a and 1b, whereas it decreases for HMW peak. Figure 1c depicts results of Monte Carlo simulations using the value of the dissociation constant $K_D = 10^{-6}$ mol/L, the ionization constant $K_I = 10^{-5}$ mol^{-1}·L, and the ionization rate constant $k_i = 10^2$ mol^{-1}·L·s^{-1}. It can be clearly seen that although ions and ion pairs have the same reactivities, bimodal MWD is obtained. The low molecular weight peak increases progressively with conversion. The number average degree of polymerization for LMW peak increases from DP = 1.5−4.6 and to 9.8 with conversion (10%, 50%, and 90%, respectively). Polydispersity of the LMW peak stays fairly narrow (M_w/M_n = 1.26, 1.21, and 1.09, respectively).

The HMW peak shifts slightly down, and its number average degree of polymerization decreases from DP = 1029 to 750 and to 460 with conversion. Polydispersities broadens from M_w/M_n = 2.24 and 2.04 to 2.54, respectively.

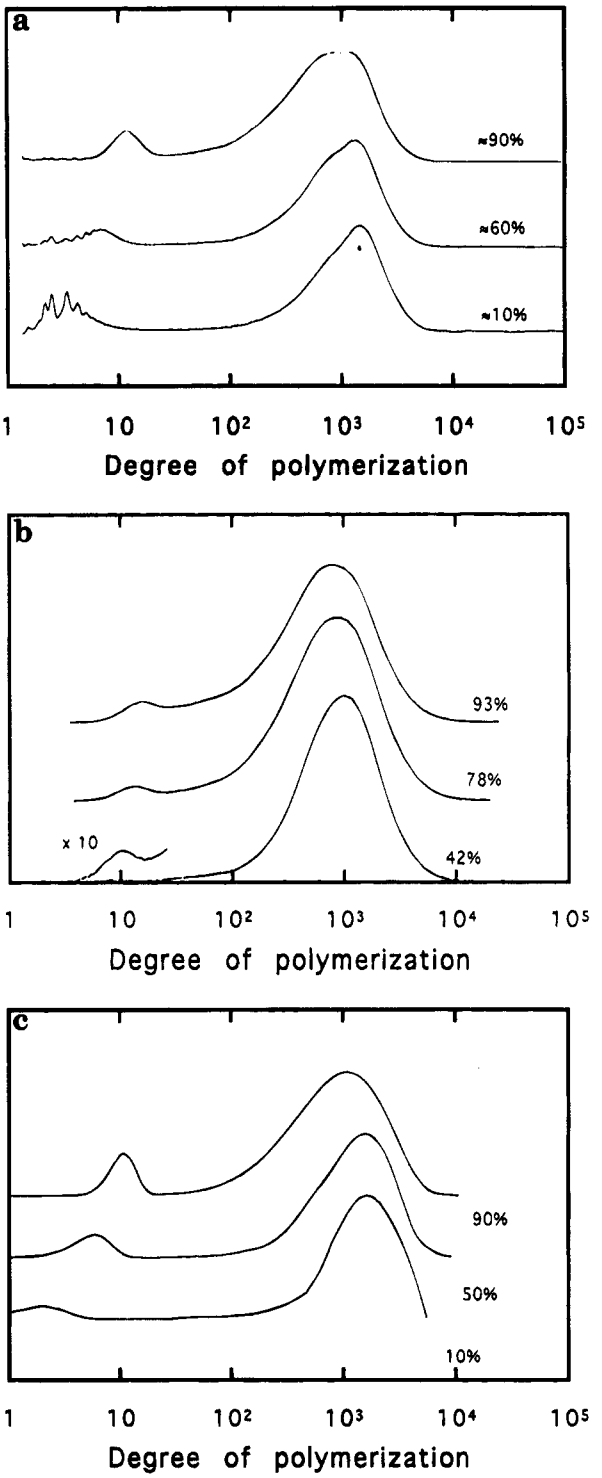

Figure 1. (a) MWD in the cationic polymerization of styrene at −20 °C in CH_2Cl_2 as a function of conversion: $[M]_o$ = 1 M, $[CH_3CH(Ph)Cl]_o$ = 0.01 M, $[SnCl_4]_o$ = 0.1 M. (b) MWD in the cationic polymerization of styrene at −20 °C in CH_2Cl_2 as a function of conversion: $[M]_o$ = 1 M, $[CH_3CH(Ph)Cl]_o$ = 0.01 M, $[BCl_3]_o$ = 0.1 M. (c) MWD in cationic polymerization as a function of conversion: $[M]_o$ = 1 M, $[I]_o$ = 0.01 M, $[LA]_o$ = 0.1 M; $k_p^+ = k_p^\bullet = 10^5$ M^{-1} s^{-1}; $K_D = 10^{-6}$ M; $K_I = 10^{-5}$ M^{-1}; $k_i = 10^2$ M^{-1} s^{-1} (system 19 in Table 1).

The overall number average degrees of polymerization increase from DP = 17 to 49 and 90. Only at the lowest conversion a value higher than the ratio of the concentrations of reacted monomer to introduced initiator is found. This means that initiation is completed at low conversion. Overall polydispersities decrease from M_w/M_n = 124 to 28 and to 12, respectively.

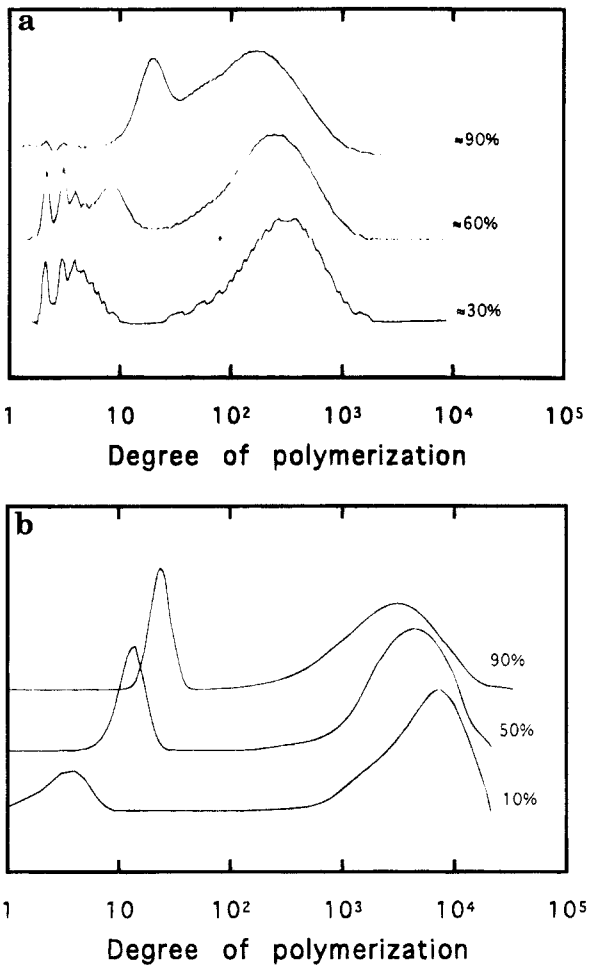

Figure 2. (a) MWD in cationic polymerization of styrene at +20 °C in CH_2Cl_2 as a function of conversion: $[M]_o = 1$ M, $[CH_3CH(Ph)Cl]_o = 0.01$ M, $[SnCl_4]_o = 0.1$ M. (b) MWD in cationic polymerization as a function of conversion: $[M]_o = 1$ M, $[I]_o = 0.01$ M, $[LA]_o = 0.1$ M; $k_p^+ = k_p^\pm = 10^5$ M^{-1} s^{-1}; $K_D = 10^{-7}$ M; $K_I = 10^{-5}$ M^{-1}; $k_i = 10^2$ M^{-1} s^{-1} (system 7).

It was not possible to experimentally detect any LMW peak at 10% conversion, since dimers or trimers are probably soluble in methanol and could not be precipitated. The proportion and a degree of polymerization of LMW increases progressively with conversion and a degree of polymerization of HMW slightly decreases. The maximum value of HMW in real systems is often controlled by transfer. This is clearly seen in Figure 2a which represents the results of the polymerization at +20 °C with all other conditions the same as in Figure 1a. The LMW peak is higher, and it progressively increases with conversion. On the other hand, the HMW peak is now centered at DP ≈ 200 rather than at DP ≈ 1000 as shown in Figure 1a for polymerization at −20 °C. Transfer must be responsible for this behavior.

Since we have not included transfer in our simulations, the closest comparison of results shown in Figure 2a might be with a system similar to that shown in Figure 1c but with 10 times lower values of K_D (dissociation is usually exothermic). In Figure 2b low molecular weight peak increases progressively with conversion from DP = 3.2 to 12.2 and to 22.8, respectively. Polydispersity of LMW peak stays fairly narrow ($M_w/M_n = 1.15$, 1.1, and 1.05, respectively). The HMW peak shifts slightly down, and its number average degree of polymerization decreases from DP = 2900 to 2300 and to 1330 with conversion. Polydispersities broaden from $M_w/M_n = 2.2$ and 2.1 to 2.78, respectively.

The overall number average degrees of polymerization slightly increases from DP = 12 to 51 and 91, as expected from the ratio of the concentrations of the reacted monomer to that of the introduced initiator. Overall polydispersities decrease from $M_w/M_n = 400$ to 70 and to 30, respectively.

Molecular weights of LMW peak increase with conversion as observed experimentally in many other cases.[5,6,18] A decrease of molecular weight of the HMW peak was also reported for other systems, and it might be ascribed to the decrease of the concentration of monomer and, consequently, reduction of the rate of propagation (first order in monomer) to that of deactivation (association of counterions and subsequent recombination) which is zero order in monomer.[6,10]

The separation of low oligomers in Figures 1a and 2a is enhanced in comparison with the simulated curves. It must be noted that the response of RI and UV detectors in SEC traces of these oligomers may not precisely reflect their concentration.

Effect of the Ionization Rates and Ionization Equilibrium Constants. Figure 3 demonstrates the effect of the ionization equilibrium on polydispersities at 90% conversion and at the constant value of $K_D = 10^{-6}$ mol/L. When ionization increases, MWD decreases and peaks tend to merge. There are two phenomena responsible for the observed changes. First is the value of the ionization equilibrium constant which sets the amount of ionic species *and* the proportion between ions and ion pairs which determines the ratio of HMW and LMW fractions. The proportion of ion pairs increases from 1% to 10% and to 50% when K_I increases from 10^{-7} to 10^{-5} and to 10^{-3} mol^{-1}·L. This effect is responsible mostly for the decrease of polydispersities from $M_w/M_n = 74$ to 12 and to 1.6, respectively. In the first system, it would be very easy to omit the LMW fraction which can be seen only after the 20-fold magnification.

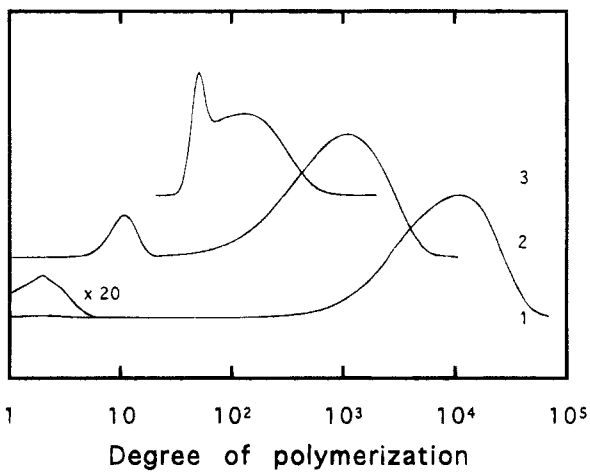

Figure 3. MWD in cationic polymerization as a function of ionization equilibrium and rate constants at 90% conversion: $[M]_o = 1$ M, $[I]_o = 0.01$ M, $[LA]_o = 0.1$ M; $k_p^+ = k_p^\pm = 10^5$ M^{-1} s^{-1}; $k_r = 10^7$ s^{-1}; $K_D = 10^{-6}$ M. **1**: $K_I = 10^{-7}$ M^{-1}; $k_i = 10^0$ M^{-1} s^{-1}. **2**: $K_I = 10^{-5}$ M^{-1}; $k_i = 10^2$ M^{-1} s^{-1}. **3**: $K_I = 10^{-3}$ M^{-1}; $k_i = 10^4$ M^{-1} s^{-1} (systems 15, 19, 23, respectively).

The second effect is related to the values of the rate constant of ionization. Because the ionization of covalent species does not depend on the polymerization degree, the ionization rate constant is related to the initiation rate constant. When the rate of ionization is very low, then incomplete initiation is observed, molecular weights are much too high, and LMW is not yet developed. In the case of the slowest initiation, a degree

of polymerization was $DP_n = 150$ rather than 90, as expected for the complete initiation at 90% conversion.

It seems that the rate of the recombination does not affect strongly the overall polydispersities for systems with bimodal MWD. It rather determines shape of LMW peak which is formed by the ion pairs which exchange with covalent species. The rate of the recombination becomes very important for systems with common ions (cf. Figures 6b, 7b, and 8b). On the other hand, if recombination is not fast enough, then the LMW fraction is not formed at all as shown in Figure 4. The overall polydispersities in case 1 are lower ($M_w/M_n = 4.8$) than in cases 2–4 ($M_w/M_n \approx 12$). However, the overall number average molecular weight is for case 1 five times higher ($DP_n \approx 490$) than in the other three cases ($DP_n \approx 90$). This indicates that once ion pairs are formed (slowly), they dissociate to free ions which propagate and terminate by the association and recombination at the macromolecular state but not at the stage of the oligomers. The rate of propagation is 100 times faster than that of recombination within ion pair. This results in the escape of free ion. In fact, all monomer is consumed when only 20% of the initiator reacted.

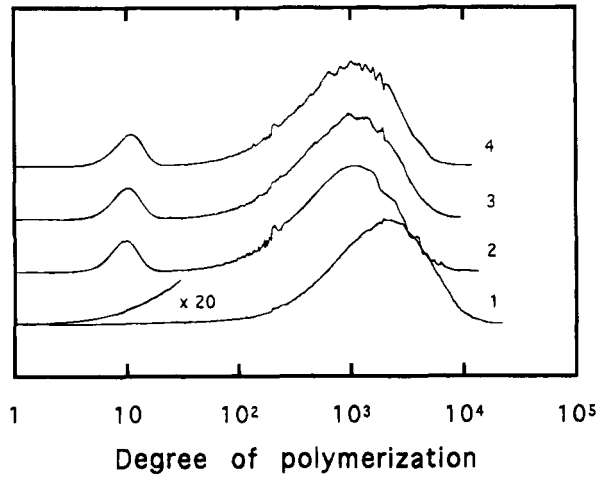

Figure 4. MWD in cationic polymerization as a function of ionization and recombination rate constants at 90% conversion: $[M]_o = 1$ M, $[I]_o = 0.01$ M, $[LA]_o = 0.1$ M; $k_p^+ = k_p^\pm = 10^5$ M^{-1} s^{-1}; $K_D = 10^{-6}$ M; $K_I = 10^{-5}$ M^{-1}. **1**: $k_i = 10^{-2}$ M^{-1} s^{-1}; $k_r = 10^3$ s^{-1}. **2**: $k_i = 10^0$ M^{-1} s^{-1}; $k_r = 10^5$ s^{-1}. **3**: $k_i = 10^2$ M^{-1} s^{-1}; $k_r = 10^7$ s^{-1}. **4**: $k_i = 10^4$ M^{-1} s^{-1}; $k_r = 10^9$ s^{-1} (systems 17, 18, 19, respectively).

Effect of the Ionization and Dissociation Equilibrium Constants. Figure 5 shows the effect of both ionization and dissociation equilibrium constants on MWD of polymers at 90% conversion with the standard recombination rate $k_r = 10^7$ mol^{-1}·L·s^{-1}. Bottom three traces and top three traces reflect the change in K_D from 10^{-5} to 10^{-6} and to 10^{-7} mol/L for two different ionization equilibrium constants $K_I = 10^{-5}$ (bottom) and 10^{-3} mol^{-1}·L (top), respectively.

When ionization is weak, a clear bimodal MWD is observed. The concentration of ion pairs equals $[C^\pm] = 10^{-8}$ mol/L, whereas the concentration of free ions increases from $[C^+] = 0.3 \times 10^{-7}$ to 10^{-7} and to 3×10^{-7} mol/L. This means that the contribution of ion pairs decreases from ≈24% to 10% and to 3%, respectively. This is seen in the relative proportions of HMW and LMW peaks.

For the stronger ionization (three top traces), the concentration of ion pairs equals $[C^\pm] = 10^{-6}$ mol/L, and the concentration of free ions varies from $[C^+] = 0.3 \times 10^{-6}$ and to 3×10^{-6} mol/L. This means that contribution of free ion increases from ≈25% to 50% and to 75%, correspondingly. In traces 4, the 25% contribution of free ions can hardly be seen without magnification (broad MWD). In traces 5 nearly equal proportions of both peaks are seen, whereas in traces 6, free ions dominate but differences between polymerization degrees are so small that peaks cannot be separated.

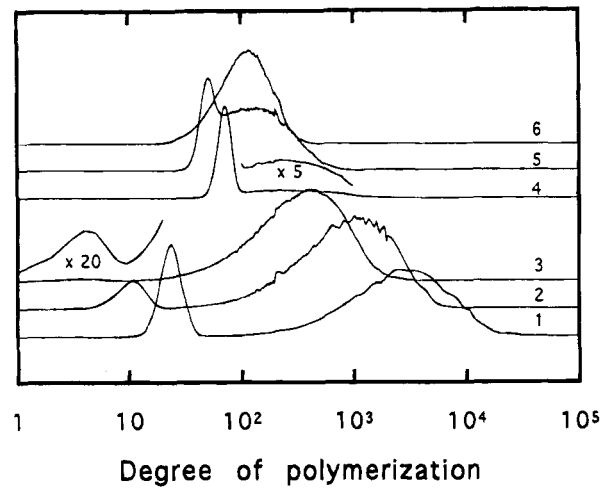

Figure 5. MWD in cationic polymerization as a function of dissociation and ionization equilibrium constants at 90% conversion: $[M]_o = 1$ M, $[I]_o = 0.01$ M, $[LA]_o = 0.1$ M; $k_p^+ = k_p^\pm = 10^5$ M^{-1} s^{-1}; $k_r = 10^7$ s^{-1}. **1**: $K_D = 10^{-7}$ M, $K_I = 10^{-5}$ M^{-1}. **2**: $K_D = 10^{-6}$ M, $K_I = 10^{-5}$ M^{-1}. **3**: $K_D = 10^{-5}$ M, $K_I = 10^{-5}$ M^{-1}. **4**: $K_D = 10^{-7}$ M, $K_I = 10^{-3}$ M^{-1}. **5**: $K_D = 10^{-6}$ M, $K_I = 10^{-3}$ M^{-1}. **6**: $K_D = 10^{-5}$ M, $K_I = 10^{-3}$ M^{-1} (systems 7, 19, 31, 11, 23, 35, respectively).

The fraction of LMW peak is determined by the proportion of ion pairs among all carbocations. However, if they exchange very rapidly with covalent species they cannot be distinguished from the dormant species and the average DP of LMW is in that case defined by the ratio of the concentrations of the reacted monomer to that of covalent species (approximately equal to that of the initiator, provided that initiation is complete). Thus, DP of LMW equals

$$DP_L = \Delta[M]/([I]_o - [I])\{[C^\pm]/([C^+] + [C^\pm])\} \quad (2)$$

Molecular weight of this fraction progressively grows with conversion and MWD is narrow ($M_w/M_n < 1.2$), if recombination of counterions within ion pair is fast enough.

DP of the HMW fraction is more difficult to estimate. DP formed during one activation period depends on the relative rates of propagation and deactivation of free ions (the association process):

$$\begin{aligned} DP_H &= (R_p/R_{assoc})\{[C^+]/([C^+] + [C^\pm])\} \\ &= \{k_p[M]/(k_{assoc}[C^+])\}\{[C^+]/([C^+] + [C^\pm])\} \\ &= k_p[M]/\{k_{assoc}([C^+] + [C^\pm])\} \end{aligned} \quad (3)$$

It is a surprising result that DP of HMW does not depend on the concentration of free ions rather than on the total amount of ionic species. However, Figure 5 shows that behavior quite clearly. The decrease of DP in traces 1–3 is due to the increase of the total concentration of carbocations from 4×10^{-8} to 1.1×10^{-7} and to 3.3×10^{-7} mol/L. The values of DP_H in traces 1–3 are in good agreement with those predicted from eq 3, assuming one single activation process for this fraction: $DP_H = 1300$, 500, 200. On the other hand, in traces 4–6 values of DP_H are in the range 100–200 and are much higher than those predicted for one single

activation for this population: DP = 80, 20, and 12, respectively. This indicates that HMW population must grow with conversion in contrast to the changes shown in Figures 1 and 2. The repetitive activation processes also lead to the more narrow MWD for this fraction which in traces 6 is $M_w/M_n = 1.30$ for the common peak of both free ions (75%) and ion pairs (25%).

Effect of Salts with Common Anion. It has been reported in the literature that the addition of salts with common ions considerably reduces polydispersities and provides well-defined systems.[8,19,21] Figure 6a,b shows the simulated effect of a common ion on evolution of molecular weights with conversion. All concentrations and rate and equilibrium constants are identical to those in Figure 1c, but the amount of counterion is $[A^-] = 10^{-6}$ and 10^{-5} mol/L, respectively. Common anions reduce the proportion and lifetime of free ions and decrease the area and DP_n of the HMW peak. Concentrations of ions and ion pairs equal $[C^{\pm}] \approx 10^{-8}$ mol/L and $[C^+] \approx 10^{-7}$ mol/L when no salt is present (Figure 1c). This corresponds to 10% population of LMW peak. When the concentration of common anion is increased to $[A^-] = 10^{-6}$ and 10^{-5} mol/L, then the concentration of the ion pairs stays the same but the concentration of free carbocations reduces to $[C^+] \approx 10^{-8}$ mol/L and $\approx 10^{-9}$ mol/L, respectively. This corresponds to 50% and 90% population of the LMW peak. The HMW peak even starts to grow with conversion and polymerization resembles an ideal case with MWD close to the Poisson distribution in Figure 6b.

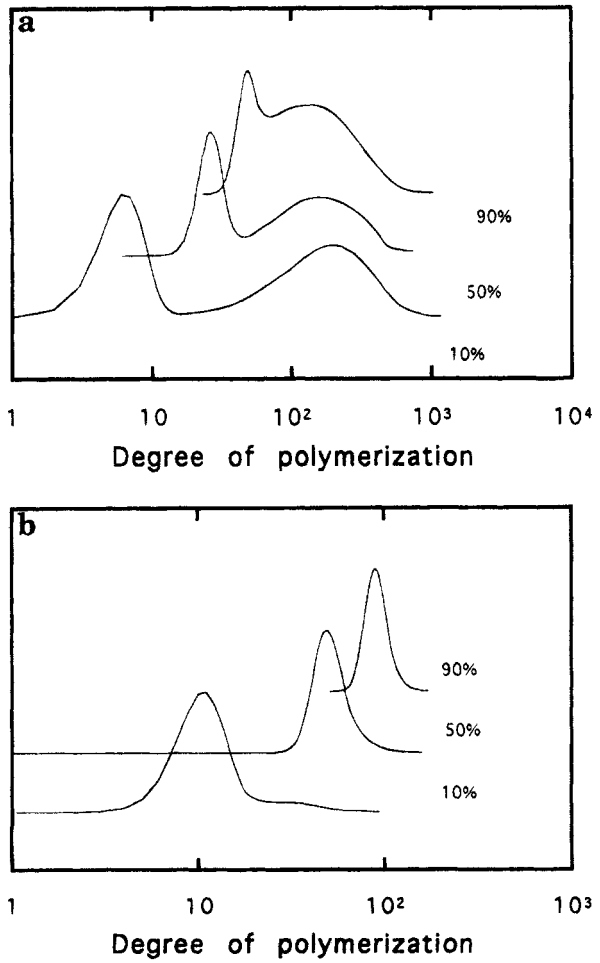

Figure 6. (a) MWD in cationic polymerization as a function of conversion in the presence of common anion: $[M]_o = 1$ M, $[I]_o = 0.01$ M, $[LA]_o = 0.1$ M; $[A^-]_o = 10^{-6}$ M; $k_p^+ = k_p^{\pm} = 10^5$ M^{-1} s^{-1}; $K_D = 10^{-6}$ M; $K_I = 10^{-5}$ M^{-1}; $k_i = 10^2$ M^{-1} s^{-1}; $k_r = 10^7$ s^{-1} (conditions as in Figure 1c except for the common anion). (b) MWD in cationic polymerization as a function of conversion in the presence of common anion: $[M]_o = 1$ M, $[I]_o = 0.01$ M, $[LA]_o = 0.1$ M; $[A^-]_o = 10^{-5}$ M; $k_p^+ = k_p^{\pm} = 10^5$ M^{-1} s^{-1}; $K_D = 10^{-6}$ M; $K_I = 10^{-5}$ M^{-1}; $k_i = 10^2$ M^{-1} s^{-1}; $k_r = 10^7$ s^{-1} (conditions as in Figure 1c except for the common anion).

A similar situation is shown in Figure 7a,b for a system with stronger ionization and stronger dissociation. Relatively broad peaks which grow with conversion are transformed to the ideal living system by the action of common ion ($[A^-] = 10^{-4}$ mol/L). Polydispersities are $M_w/M_n = 1.12$ ($DP_n = 10$), 1.02 ($DP_n = 50$), and 1.01 ($DP_n = 100$) at 10, 50 and 90% conversion as predicted by Poisson distribution. The MWD at 10% conversion without salt was clearly bimodal as shown in Figure 7a.

It is possible that oxonium ions are formed in the presence of small amounts of adventitious moisture. In that case, the accompanying anions may act apparently in the same way as purposely added salts with common ions.

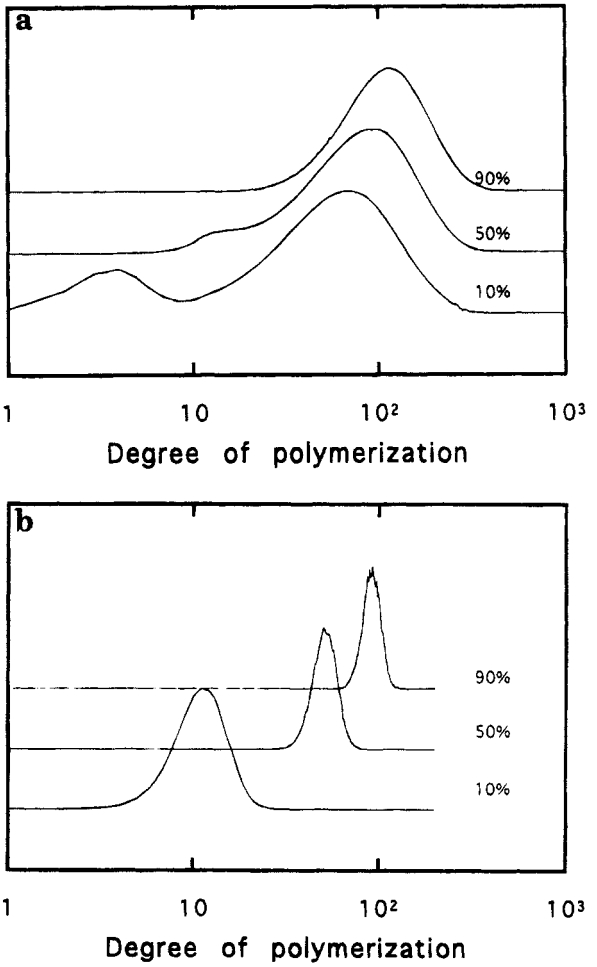

Figure 7. (a) MWD in cationic polymerization as a function of conversion in the presence of common anion (*no salt added*): $[M]_o = 1$ M, $[I]_o = 0.01$ M, $[LA]_o = 0.1$ M; $[A^-]_o = 0$ M ($[A^-] = [C^+] = 3 \times 10^{-6}$ *M*); $k_p^+ = k_p^{\pm} = 10^5$ M^{-1} s^{-1}; $K_D = 10^{-5}$ M; $K_I = 10^{-3}$ M^{-1}; $k_i = 10^4$ M^{-1} s^{-1}; $k_r = 10^7$ s^{-1} (conditions as in Figure 5, trace 6; system 35). (b) MWD in cationic polymerization as a function of conversion in the presence of common anion: $[M]_o = 1$ M, $[I]_o = 0.01$ M, $[LA]_o = 0.1$ M; $[A^-]_o = 10^{-4}$ M; $k_p^+ = k_p^{\pm} = 10^5$ M^{-1} s^{-1}; $K_D = 10^{-5}$ M; $K_I = 10^{-3}$ M^{-1}; $k_i = 10^4$ M^{-1} s^{-1}; $k_r = 10^7$ s^{-1} (conditions as in Figure 7a, except for added salt).

Effect of the Dynamics of Ionization. When only one single peak is observed, then the dynamics of ionization become more important. Figure 8a,b shows the progressive broadening of MWD with the decrease

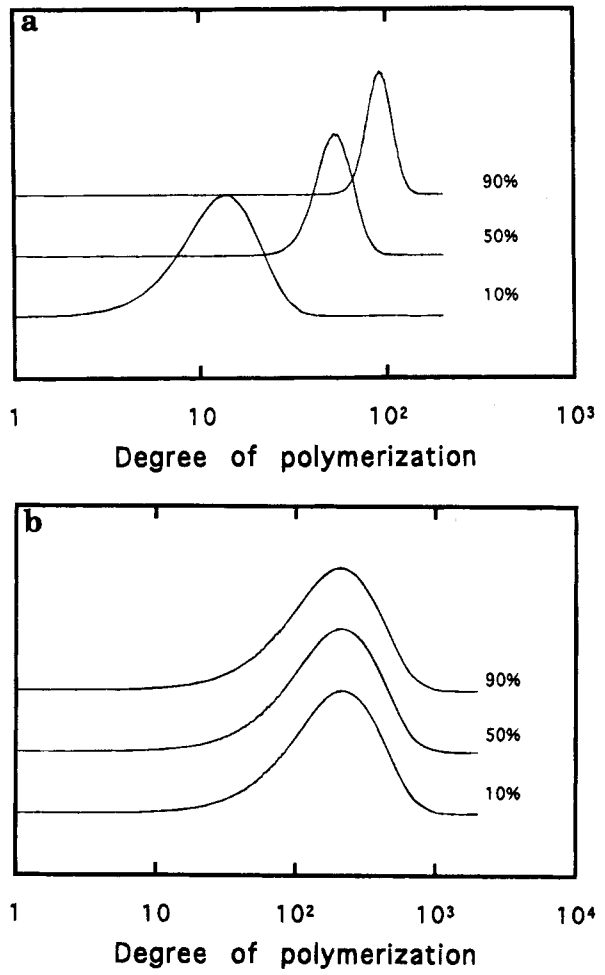

Figure 8. (a) MWD in cationic polymerization as a function of conversion in the presence of common anion: $[M]_o = 1$ M, $[I]_o = 0.01$ M, $[LA]_o = 0.1$ M; $[A^-]_o = 10^{-4}$ M; $k_p^+ = k_p^\pm = 10^5$ M^{-1} s^{-1}; $K_D = 10^{-5}$ M; $K_I = 10^{-3}$ M^{-1}; $k_i = 10^2$ M^{-1} s^{-1}; $k_r = 10^5$ s^{-1} (dynamics of ionization 10^2 times slower than shown in Figure 7b; conditions as in system 34, except for the common anion). (b) MWD in cationic polymerization as a function of conversion in the presence of common anion: $[M]_o = 1$ M, $[I]_o = 0.01$ M, $[LA]_o = 0.1$ M; $[A^-]_o = 10^{-4}$ M; $k_p^+ = k_p^\pm = 10^5$ M^{-1} s^{-1}; $K_D = 10^{-5}$ M; $K_I = 10^{-3}$ M^{-1}; $k_i = 10^0$ M^{-1} s^{-1}; $k_r = 10^3$ s^{-1} (dynamics of ionization 10^4 times slower than shown in Figure 7b; conditions as in system 33, except for the common anion).

of the rate constants of ionization and recombination of counterions. Values of equilibrium constants of ionization and dissociation as well as the concentration of common ion are exactly the same as in Figure 7b. Traces 8a are simulated for the system with 100 times slower exchange reactions than those in Figure 7b. They show a relatively small additional broadening of MWD in comparison with those in Figure 7b (M_w/M_n = 1.31, 1.05, and 1.025 in comparison with 1.12, 1.02, and 1.01 at 10, 50, and 90% conversion, respectively). Number average molecular weights correspond very well to those for fast initiation (DP_n = 10, 50, and 90 for both systems).

However, traces shown in Figure 8b are dramatically different. When the dynamics of ionization is slowed down 100 more times (thus, 10^4 times slower than for the system from 7b), polydispersities and molecular weights are very far from the ideal behavior: DP_w/DP_n = 1.99, 2.00, and 2.04 and DP_n = 110, 108, and 104 at 10, 50, and 90% conversion. Thus, initiation is not completed even at 90% monomer conversion and polydispersities are very broad. At first glance this system could be identified as a transfer dominated one, but no transfer is present. This system is *living* in the purist's sense. No transfer and no (irreversible) termination takes place. The polymerization degree in this system is determined by the ratio of the concentration of the reacted monomer to that of the reacted initiator. At the same time DP_n depends on the ratio of the rate of propagation to that of deactivation of ion pairs:

$$DP_n = R_p/R_r = k_{p^\pm}[M][C^\pm]/(k_r[C^\pm]) \approx 100 \quad (4)$$

This polymerization degree is observed already at 10% conversion which indicates that only 10% of initiator was consumed at this stage.

Polydispersities increase with the ratio of rate of propagation to that of deactivation of growing species.[21-23] Figures 9 and 10 show the calculated changes of the MWD with conversion and as a function of the polymerization degree for systems with only ion pairs and inactive covalent species. This is the case of systems with common ions when free ions are suppressed. MWD is unimodal but its breadth depends on the ratio of the rate constants of propagation and recombination of the ion pairs (k_p/k_r). Changes of MWD with conversion (p) shown in Figure 9 confirm to the following equation obtained by the modification of the expression from ref 23:

$$DP_w/DP_n = 1 + 1/DP_n + ([I]_o - [I])(k_p/k_r)(2 - p)/p \quad (5)$$

Nearly constant values of $M_w/M_n \approx 2$ in Figure 8b are in good agreement with eq 5. Parameter c ($c = ([I]_o -$

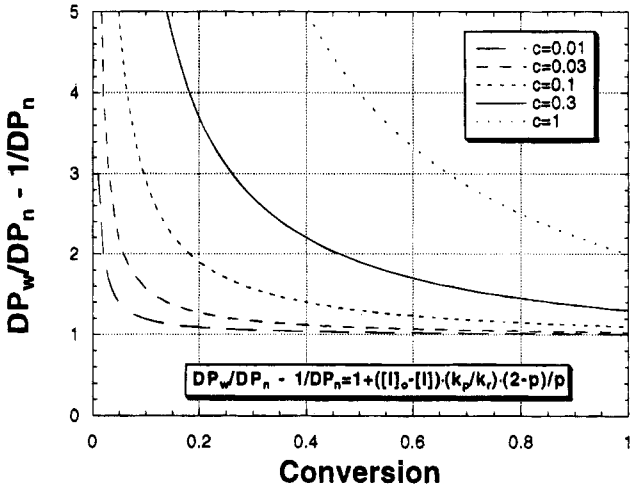

Figure 9. Effect of parameter $c = ([I]_o - [I])(k_p/k_r)$ on evolution of polydispersities with conversion.

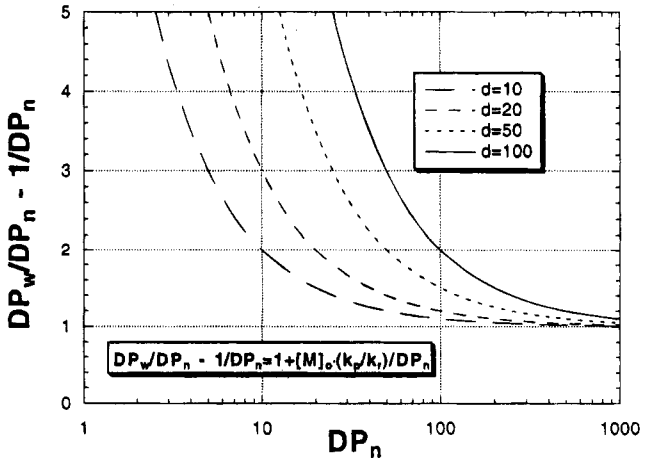

Figure 10. Effect of parameter $d = [M]_o(k_p/k_r)$ on evolution of polydispersities with chain length at complete conversion.

$[I])(k_p/k_r)$) varies with conversion and equals $c \approx 1$ at 90% conversion, $c \approx 0.5$ at 50% conversion, and $c \approx 0.1$ at 10% conversion (only 10% of initiator is consumed in the latter case).

In plots shown in Figure 9, polydispersities continuously decrease with conversion and with the increase of the chain length in contrast to systems dominated by transfer. When exchange is slow, a number of exchange events is higher during the buildup of a longer chain, leading to more uniform distribution. At the lower concentration of growing species ($[I]_o - [I]$), longer chains with more narrow MWD can be formed. Figure 10 demonstrates how polydispersities are affected by chain lengths at complete conversion. In order to obtain polymers with lower polydispersities, longer chains have to be formed if deactivation is slow. At complete conversion, polydispersities are defined by the following equation:

$$DP_w/DP_n = 1 + 1/DP_n + [M]_o(k_p/k_r)/DP_n \quad (6)$$

It may happen in real systems that transfer will start to operate at such high molecular weights and polydispersities may initially decrease but then they may start to increase again.

Conclusions

The calculations and the simulations shown in this work confirm the following phenomena:

(1) Bimodal MWD is formed in systems with free ions and ion pairs of identical reactivities but different lifetimes. This is possible when conversion to dormant species (covalent) proceeds with different rates. It is not necessary to assume different reactivities of ions and ion pairs, and it is not necessary to assume covalent propagation.

(2) The ratio of HMW to LMW peak depends on the ratio of concentrations of free ions and ion pairs, provided the reactivation of HMW does not contribute significantly. If the reactivities of free ions and ion pairs are different it is necessary to use the weighted product of proportion and reactivity to estimate the contribution of each fraction.

(3) In most systems the HMW fraction formed with free ions is generated during one activation period. In that case MW of this fraction decreases with conversion and is defined by the ratio of rates of propagation to association. At high concentration of free ions (or in the presence of common anions) the association becomes very fast and the HMW fraction may be formed in a few activation steps. In that case this fraction may grow with conversion (both M_n and contribution) and a more narrow MWD may be observed ($M_w/M_n < 2$).

(4) The LMW fraction is formed by ion pairs. Concentration of these chains is roughly equal to that of the introduced initiator, provided that initiation is completed and the reactivation of HMW fraction can be neglected. Nearly all of these chains are in the dormant state. They reversibly ionize, and a small fraction escapes as free ions to HMW fraction. The chance that chains in HMW fraction ionize again is usually small because it consists of a very small number of chains.

(5) In calculations no transfer reaction was considered so the limit of the growth of both fractions is simply due to the monomer consumption. In real systems, transfer may limit the HMW fraction, depending on monomer and temperature.

(6) Dynamics of the dissociation is very important for the evolution of MW. If the association of free ions is fast, then they can grow together with ion pairs. The increase of the anion's concentration will not only reduce lifetime of free ions but also their ratio to ion pairs and relative proportion of HMW and LMW peaks.

(7) Dynamics of ionization is important, too. The rate of deactivation (recombination of counterions to covalent species) sets the lifetime of ion pairs and affects the MWD of the LMW peak. If recombination is much slower than propagation, the LMW peak may not be formed at all. Slow ionization may lead to a very high MW if initiation is incomplete. This also requires the recombination process to be slow enough.

Experimental Section

Computations were performed on 486 PC 60 MHz computer. The Episode integration method for stiff systems (program Scientist from Micromath Scientific) was used for numerical integrations. The Monte Carlo simulations were carried out using a program written in TurboPascal v. 6.0.

Styrene was washed with 10% aqueous NaOH and then with water, dried overnight over KOH pellets, and distilled twice over CaH_2 before use. CH_2Cl_2 was washed with fuming acid until the acid layer remained colorless, washed with aqueous $NaHCO_3$ and with distilled water, dried over $CaCl_2$, and distilled once from P_2O_5 and twice from CaH_2 under vacuum. Tetra-*n*-butylammonium chloride was dried under high vacuum. 1-Phenylethyl chloride, $SnCl_4$, and BCl_3 (1 mol/L solution in CH_2Cl_2) were used as received (Aldrich). Polymerizations were carried out under argon in baked Schlenk flasks, capped with rubber septa. After a certain interval, they were terminated by the addition of a methanol–ammonia mixture 95–5 (v/v). The quenched reaction mixture was washed successively with dilute hydrochloric acid, dilute NaOH, and water until neutral, in order to remove the salt and the initiator residues. The conversion of styrene was determined gravimetrically after the evaporation of the solvent and the remaining monomer under vacuum.

Acknowledgment. This work was partially supported by the donors of the Petroleum Research Fund administered by the American Chemical Society, by the National Science Foundation, and by matching funds from DuPont, PPG Industries, and Xerox.

Appendix

Numerical Integrations. The following set of general differential equations has been used for the numerical integrations. In simulations described in this paper $k_p^c = 0$.

$$d[C_0]/dt = -k_i[C_0][LA] + k_r[C^{\pm}{}_0] - k_p^c[C_0][M] \quad (A1)$$

$$d[C_i]/dt = -k_i[C_i][LA] + k_r[C^{\pm}{}_i] - k_p^c[C_i][M] + k_p^c[C_{i-1}][M] \quad (i > 0) \quad (A2)$$

$$d[C^{\pm}{}_0]/dt = k_i[C_0][LA] - k_r[C^{\pm}{}_0] - k_p^{\pm}[C^{\pm}{}_0][M] - k_{diss}[C^{\pm}{}_0] + k_{assoc}[C^+{}_0][A^-] \quad (A3)$$

$$d[C^{\pm}{}_i]/dt = k_i[C_i][LA] - k_r[C^{\pm}{}_i] - k_p^{\pm}[C^{\pm}{}_i][M] + k_p^{\pm}[C^{\pm}{}_{i-1}][M] - k_{diss}[C^{\pm}{}_0] + k_{assoc}[C^+{}_i][A^-] \quad (i > 0) \quad (A4)$$

$$d[C^+{}_0]/dt = k_{diss}[C^{\pm}{}_0] - k_{assoc}[C^+{}_0][A^-] - k_p^+[C^+{}_0][M] \quad (A5)$$

$$d[C^+_i]/dt = k_{diss}[C^{\pm}_i] - k_{assoc}[C^+_i][A^-] - k_p^+[C^+_i][M] + k_p^+[C^+_{i-1}][M] \quad (i > 0) \quad \text{(A6)}$$

$$d[M]/dt = -k_p^c[M]\sum_{i=0}^{\infty}[C_i] - k_p^{\pm}[M]\sum_{i=0}^{\infty}[C^{\pm}_i] - k_p^+[M]\sum_{i=0}^{\infty}[C^+_i] \quad \text{(A7)}$$

([LA] was much higher than the concentration of active species and was assumed to be constant.)

The corresponding equations for moments of distribution for populations formed by covalent species (c), ion pairs (p), and free ions (f) have been obtained by combination of the above equations. Distribution moments μ of 0, 1, and 2 order have been calculated:

$$d\mu_{c0}/dt = d\sum_{i=0}^{\infty}[C_i]/dt = d[C]/dt = -k_i[LA][C] + k_r[C^{\pm}] \quad \text{(A8)}$$

$$d\mu_{c1}/dt = d\sum_{i=0}^{\infty} i[C_i]/dt = -k_i[LA]\mu_{c1} + k_r\mu_{p1} + k_p^c[M][C] \quad \text{(A9)}$$

$$d\mu_{c2}/dt = d\sum_{i=0}^{\infty} i^2[C_i]/dt = -k_i[LA]\mu_{c2} + k_r\mu_{p2} + k_p^c[M]([C] + 2\mu_{c1}) \quad \text{(A10)}$$

$$d\mu_{p0}/dt = d\sum_{i=0}^{\infty}[C^{\pm}_i]/dt = d[C^{\pm}]/dt = k_i[LA][C] - k_r[C^{\pm}] + k_{assoc}[C^+][A^-] - k_{diss}[C^{\pm}] \quad \text{(A11)}$$

$$d\mu_{p1}dt = d\sum_{i=0}^{\infty} i[C^{\pm}_i]/dt = k_i[LA]\mu_{c1} - k_r\mu_{p1} + k_{assoc}\mu_{f1}[A^-] - k_{diss}\mu_{p1} + k_p^{\pm}[M][C^{\pm}] \quad \text{(A12)}$$

$$d\mu_{p2}/dt = d\sum_{i=0}^{\infty} i^2[C^{\pm}_i]/dt = k_i[LA]\,\mu_{c2} - k_r\mu_{p2} + k_{assoc}\mu_{f2}[A^-] - k_{diss}\mu_{p2} + k_p^{\pm}[M]([C^{\pm}] + 2\,\mu_{p1}) \quad \text{(A13)}$$

$$d\mu_{f0}/dt = d\sum_{i=0}^{\infty}[C^+_i]/dt = d[C^+]/dt = -k_{assoc}[C^+][A^-] + k_{diss}[C^{\pm}] \quad \text{(A14)}$$

$$d\mu_{f1}/dt = d\sum_{i=0}^{\infty} i[C^+_i]/dt = -k_{assoc}\mu_{f1}[A^-] + k_{diss}\mu_{p1} + k_p^+[M][C^+] \quad \text{(A15)}$$

$$d\mu_{f2}/dt = d\sum_{i=0}^{\infty} i^2[C^+_i]/dt = -k_{assoc}\mu_{f2}[A^-] + k_{diss}\mu_{p2} + k_p^+[M]([C^+] + 2\mu_{f1}) \quad \text{(A16)}$$

where notation of the distribution moments and of total concentrations of different species is given by the left sides of the above equations. It was assumed that the equilibrium constants and the rate constants of exchange for the growing chains are identical to that for the initiator. In systems without salts with the common anion the concentration of free counterion $[A^-]$ is equal to that of free carbocations $[C^+]$ and the sum of concentrations of different species is equal to the initial concentration of initiator. Constant concentration of anion $[A^-]$ was assumed in systems with a common anion.

Consequently, the concentrations of active species and counterion can be computed from the following equations (for systems without salt):

$$[C^{\pm}] = \frac{(\Delta)^{1/2} - 1}{2(k_{assoc}/k_{diss})(1 + k_r/(k_i[LA]))} \quad \text{(A17)}$$

where $\Delta = 1 + 4(k_{assoc}/k_{diss})(1 + k_r/(k_i[LA]))[I]_0$ ($[I]_0 = [C_0]_0 + [C^{\pm}{}_0]_0 + [C^+{}_0]_0$ is the initial concentration of initiator.)

$$[C^+] = [A^-] = (k_{assoc}/k_{diss})[C^{\pm}]^2 \quad \text{(A18)}$$

$$[C] = [C^{\pm}]k_r/(k_i[LA]) \quad \text{(A19)}$$

The constant concentrations of active species make the solution of eq A7 for [M] straightforward:

$$[M] = [M]_0 \exp[-(k_p^c[C] + k_p^{\pm}[C^{\pm}] + k_p^+[C^+])t] \quad \text{(A20)}$$

Consequently, the numerical integration can be reduced to only nine equations: A2, A4, A6, A9, A10, A12, A13, A15, and A16, in which [M] is expressed as a function of time. The number average degrees of polymerization as well as the polydispersity indexes can be computed at any reaction time:

$$DP_n^c = \mu_{c1}/([C] - [C_0]) \quad \text{(A21)}$$

$$DP_n^p = \mu_{p1}/([C^{\pm}] - [C^{\pm}{}_0]) \quad \text{(A22)}$$

$$DP_n^f = \mu_{f1}/([C^+] - [C^+{}_0]) \quad \text{(A23)}$$

$$DP_n = (\mu_{c1} + \mu_{p1} + \mu_{f1})/([C] + [C^{\pm}] + [C^+] - [C_0] - [C^{\pm}{}_0] - [C^+{}_0]) \quad \text{(A24)}$$

$$Disp^c = \mu_{c2}/(\mu_{c1}\,DP_n^c) \quad \text{(A25)}$$

$$Disp^p = \mu_{p2}/(\mu_{p1}\,DP_n^{\pm}) \quad \text{(A26)}$$

$$Disp^f = \mu_{f2}/(\mu_{f1}\,DP_n^+) \quad \text{(A27)}$$

$$Disp = (\mu_{c2} + \mu_{p2} + \mu_{f2})/[(\mu_{c2} + \mu_{p2} + \mu_{f2})DP_n] \quad \text{(A28)}$$

where DP_n and Disp ($= DP_w/DP_n$) are the number average degree of polymerization and the polydispersity index of polymer, while superscripts c, p, and f indicate that the given DP_n or Disp was computed for chains terminated with the corresponding active center only. Equations for systems with salt were modified accordingly.

Monte Carlo Simulations. As a model of a polymer chain a variable pair ⟨*length*, *type*⟩ was chosen. A variable *length* corresponds to polymer length while the variable *type* corresponds to the type of the active center of growing macromolecule. The polymerization process was modeled by changing sequentially the pair ⟨*length*,

type) as many times as necessary until the variable *time* (corresponding to the polymerization time) reached the assumed value (for the desired monomer conversion). Changes of (*length*, *type*) were performed randomly with the probabilities equal to the probabilities of the corresponding reactions. The variable *time* and the monomer concentration were modified after each reaction step according to eqs A17–A20. The corresponding modifications of variables *type*, *length* and *time* are presented schematically below together with the appropriate probabilities:

covalent species:

ionization: $P_i = k_i/(k_i + k_p^c[M]) = 1$; *type* ⇒ ion pair

propagation: $P_p^c = k_p^c[M]/(k_i + k_p^c[M]) = 0$; *length* ⇒ *length* + 1

$$time \Rightarrow time - \ln(random)/(k_i + k_p^c[M])$$

ion pair:

ions combination: $P_r = k_r/(k_r + k_{diss} + k_p^{\pm}[M])$; *type* ⇒ covalent

dissociation: $P_{diss} = k_{diss}/(k_r + k_{diss} + k_p^{\pm}[M])$; *type* ⇒ free cation

propagation: $P_p^{\pm} = k_p^{\pm}[M]/(k_r + k_{diss} + k_p^{\pm}[M])$; *length* ⇒ *length* + 1

$$time \Rightarrow time - \ln(random)/(k_r + k_{diss} + k_p^{\pm}[M])$$

free cation:

association:

$P_{assoc} = k_{assoc}[A^-]/(k_{assoc}[A^-] + k_p^+[M])$; *type* ⇒ ion pair

propagation: $P_p^+ = k_p^+[M]/(k_{assoc}[A^-] + k_p^+[M])$; *length* ⇒ *length* + 1

$$time \Rightarrow time - \ln(random)/(k_{assoc}[A^-] + k_p^+[M])$$

(*random* is a uniform random number from the range (0, 1).)

The initial value of the variable *length* was zero while that of the variable *type* was set randomly with the probabilities equal to fractions of different types of active species in the modeled polymerization. After the assumed value was reached by the variable *time* the variable *chains* (initial value zero) was increased by one, "polymer length" noted by increasing by one of the corresponding element of the array *polymer*. Then the whole process was repeated the assumed number of times (number of polymer chains). At the end the MWD was computed accordingly assuming that the values of the elements of the array *polymer* are the numbers of chains of the given length.

The MWD was plotted with the horizontal axis log (DP) and the vertical axis $n_{DP}DP^2/\Sigma(n_{DP}DP^2)$, where the sum was over all polymer lengths (DP). n_{DP} is the number of polymer chain of the given DP. Such a plot resembles in the best way the GPC plots in which the vertical axis is proportional to Δ(polymer mass)/Δ(elution volume) because the polymer mass is proportional to $n_{DP}DP$, while the elution volume is usually proportional to log(DP).

References and Notes

(1) Szwarc, M. *Carbanions, Living Polymers and Electron Transfer Processes*; John Wiley & Sons: New York, 1968.
(2) Schultz, G. V. *Chem. Techn.* **1973**, 220.
(3) Figini, R. V. *Makromol. Chem.* **1967**, *107*, 170.
(4) Parsoons, A. *J. Phys. Chem.* **1974**, *71*, 127.
(5) Matyjaszewski, K.; Sigwalt, P. *Polym. Int.* **1994**, *35*, 1.
(6) Masuda, T.; Sawamoto, M.; Higashimura, T. *Makromol. Chem.* **1976**, *177*, 2995.
(7) Pepper, D. C. *J. Polym. Sci., Polym. Symp.* **1975**, *50*, 51.
(8) Dunn, D. J.; Mathias, E.; Plesch, P. H. *Europ. Polym. J.* **1976**, *12*, 1.
(9) Kennedy, J. P.; Ivan, B. *Designed Polymers by Carbocationic Macromolecular Engineering, Theory and Practive*; Hanser: Munich, 1992.
(10) Sawamoto, M.; Higashimura, T. *Makromol. Chem., Macromol. Symp.* **1992**, *60*, 47.
(11) Matyjaszewski, K.; Sigwalt, P. *Makromol. Chem.* **1986**, *187*, 2299.
(12) Matyjaszewski, K. *Makromol. Chem., Macromol. Symp.* **1988**, *13/14*, 433.
(13) Matyjaszewski, K. *J. Polym. Sci., Chem.* **1993**, *31*, 995.
(14) Mayr, H. *Angew. Chem.* **1990**, *29*, 1371.
(15) Kunitake, T.; Takarabe, K. *Macromolecules* **1979**, *12*, 1061.
(16) Vairon, J.-P.; Rives, A.; Bunel, C. *Makromol. Chem., Macromol. Symp.* **1992**, *60*, 97.
(17) Matyjaszewski, K. *Makromol. Chem., Macromol. Symp.* **1992**, *54/55*, 51.
(18) (a) Szymanski, R. Presented at the 10th IUPAC Symposium on Cationic Polymerization, Borovets, 1993. (b) Penczek, S. *Makromol. Chem., Rapid Commun.* **1992**, *13*, 147.
(19) Lin, C. H.; Xiang, J. S.; Matyjaszewski, K. *Macromolecules* **1993**, *26*, 2785.
(20) Balogh, L.; Wang, L.; Faust, R. *Macromolecules* **1994**, *27*, 3543.
(21) Ishihama, Y.; Sawamoto, M.; Higashimura, T. *Polym. Bull.* **1990**, *23*, 361.
(22) Matyjaszewski, K.; Lin, C. H. *Makromol. Chem., Macromol. Symp.* **1991**, *47*, 221.
(23) Puskas, J. E.; Kaszas, G.; Litt, M. *Macromolecules* **1991**, *24*, 5278.
(24) Kunkel, D.; Mueller, A. H. E.; Janata, M.; Lochman, L. *Makromol. Chem., Macromol. Symp.* **1992**, *60*, 315.